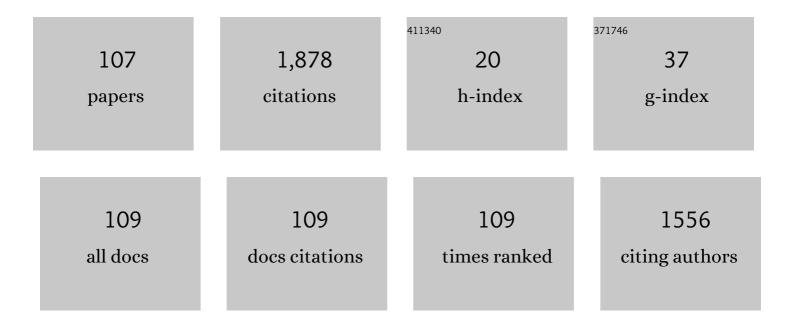
List of Publications by Year in descending order

Source: https://exaly.com/author-pdf/3818346/publications.pdf Version: 2024-02-01



YU-7HI SONC

#	Article	IF	CITATIONS
1	Wavelength-tunable 1104â€nm nonlinear amplifier loop mirror laser based on a polarization-maintaining double-cladding fiber. Optics Letters, 2022, 47, 5.	1.7	5
2	The Design of >2000-nm, â^¼100-MHz Ultrafast Tm-Doped Fiber Soliton Laser Source. Journal of Lightwave Technology, 2022, 40, 2116-2122.	2.7	10
3	A new global analytical ab initio potential energy surface for the dynamics of the C+(2P) + SH(X2Î) reaction. Physical Chemistry Chemical Physics, 2022, 24, 1007-1015.	1.3	2
4	A QM/MM study on through space charge transfer-based thermally activated delayed fluorescence molecules in the solid state. Journal of Materials Chemistry C, 2022, 10, 517-531.	2.7	30
5	Theoretical Study on the Light-Emitting Mechanism of Multifunctional Thermally Activated Delayed Fluorescence Molecules. Journal of Physical Chemistry C, 2022, 126, 2437-2446.	1.5	10
6	Structure–property relationship study of blue thermally activated delayed fluorescence molecules with different donor and position substitutions: theoretical perspective and molecular design. Journal of Materials Chemistry C, 2022, 10, 4723-4736.	2.7	17
7	Theoretical perspective of relationship between molecular structure and luminescence properties for circularly polarized thermally activated delayed fluorescence. Spectrochimica Acta - Part A: Molecular and Biomolecular Spectroscopy, 2022, 275, 121164.	2.0	6
8	Gigahertz-repetition rate, high power, ultrafast Tm-doped fiber laser source. Optics and Laser Technology, 2022, 153, 108206.	2.2	4
9	Theoretical studies on the excited-state properties of thermally activated delayed fluorescence molecules with aggregation induced emission. Journal of Materials Chemistry C, 2022, 10, 9377-9390.	2.7	7
10	Novel Deep Red Thermally Activated Delayed Fluorescence Molecule with Aggregation-Induced Emission Enhancement: Theoretical Design and Experimental Validation. Journal of Physical Chemistry Letters, 2022, 13, 4711-4720.	2.1	16
11	A theoretical perspective of the relationship between the structures and luminescence properties of red thermally activated delayed fluorescence molecules. Physical Chemistry Chemical Physics, 2022, 24, 17140-17154.	1.3	6
12	The theoretical study of excited-state intramolecular proton transfer of N, N,-bis (salicylidene)-(2-(3â€34â€2-diaminophenyl) benzothiazole). Journal of Luminescence, 2021, 230, 117741.	1.5	62
13	Design strategy for blue thermally activated delayed fluorescence: Position and methyl substitutions. Chemical Physics Letters, 2021, 764, 138260.	1.2	6
14	Theoretical insight into the vibrational excitation effect of the S+(4S)Â+ÂH2(X1â~+g) reaction. Chemical Physics Letters, 2021, 764, 138257.	1.2	1
15	Modulation of MXene Nb ₂ CT _x saturable absorber for passively Q-switched 2.85 µm Er:Lu ₂ O ₃ laser. Optics Letters, 2021, 46, 1385.	1.7	11
16	The Investigation on Ultrafast Pulse Formation in a Tm–Ho-Codoped Mode-Locking Fiber Oscillator. Molecules, 2021, 26, 3460.	1.7	6
17	Sensing mechanism of fluorescent sensor to Cu2+ based on inhibiting ultra-fast intramolecular proton transfer process. Spectrochimica Acta - Part A: Molecular and Biomolecular Spectroscopy, 2021, 254, 119685.	2.0	6
18	Accurate High-Level Ab Initio-Based Global Potential Energy Surface and Quantum Dynamics Calculation for the First Excited State of CH2+. Journal of Physical Chemistry A, 2021, 125, 5490-5498.	1.1	3

#	Article	IF	CITATIONS
19	Investigation on the optical nonlinearity of the layered magnesium-mediated metal organic framework (Mg-MOF-74). Optics Express, 2021, 29, 23786.	1.7	3
20	Systematic theoretical investigation of two novel molecules BtyC-1 and BtyC-2 based on ESIPT mechanism. Spectrochimica Acta - Part A: Molecular and Biomolecular Spectroscopy, 2021, 258, 119810.	2.0	16
21	Broadband and enhanced nonlinear optical modulation characteristics of CuBTC for pulsed lasers. Optical Materials Express, 2021, 11, 3546.	1.6	9
22	Photophysical properties of fluorescent nucleobase P-analogues expected to monitor DNA replication. Spectrochimica Acta - Part A: Molecular and Biomolecular Spectroscopy, 2021, 260, 119926.	2.0	9
23	Field-free alignment of triatomic molecules controlled by a slow turn-on and rapid turn-off shaped laser pulse. Molecular Physics, 2021, 119, e1859147.	0.8	2
24	Examining the isotope effect on CH decay and H exchange reactions: H(2S) + CH(D/T)(2Î). Physica Scripta, 2021, 96, 015404.	1.2	1
25	Intermolecular interaction on excited-state properties of fluoro-substituted thermally activated delayed fluorescence molecules with aggregation-induced emission: a theoretical perspective. Molecular Physics, 2021, 119, e1862931.	0.8	3
26	Effects of Secondary Acceptors on Excited-State Properties of Sky-Blue Thermally Activated Delayed Fluorescence Molecules: Luminescence Mechanism and Molecular Design. Journal of Physical Chemistry A, 2021, 125, 175-186.	1.1	12
27	Potential energy curves, spectroscopic constants, and vibrational energy levels of CS ⁺ (<i>X</i> ² Σ ⁺ / <i>A</i> ² Î). Molecular Physics, 2020, 118, .	0.8	4
28	Thermally activated delayed fluorescence emitters with dual conformations for white organic light-emitting diodes: mechanism and molecular design. Physical Chemistry Chemical Physics, 2020, 22, 1313-1323.	1.3	20
29	Theoretical perspective for luminescent mechanism of thermally activated delayed fluorescence emitter with excited-state intramolecular proton transfer. Journal of Materials Chemistry C, 2020, 8, 98-108.	2.7	27
30	Substitution effect on luminescent property of thermally activated delayed fluorescence molecule with aggregation induced emission: A QM/MM study. Spectrochimica Acta - Part A: Molecular and Biomolecular Spectroscopy, 2020, 229, 117964.	2.0	15
31	Suppression of aggregation caused quenching in U-shaped thermally activated delayed fluorescence molecules: Tert-butyl effect. Journal of Luminescence, 2020, 219, 116899.	1.5	20
32	State-to-state dynamics of S+(2D)Â+ÂH2(X1Σg+)(v, j) collision reaction based on the H2S+ (X 2A′′)potenti energy surface. Computational and Theoretical Chemistry, 2020, 1191, 113021.	al 1.1	1
33	Theoretical Study on Thermally Activated Delayed Fluorescence Emitters in White Organic Light-Emitting Diodes: Emission Mechanism and Molecular Design. Journal of Physical Chemistry A, 2020, 124, 7526-7537.	1.1	14
34	Solid-state effect on luminescent properties of thermally activated delayed fluorescence molecule with aggregation induced emission: A theoretical perspective. Spectrochimica Acta - Part A: Molecular and Biomolecular Spectroscopy, 2020, 241, 118634.	2.0	11
35	A global potential energy surface for the ground electronic state of SSiH. Journal of Physics B: Atomic, Molecular and Optical Physics, 2020, 53, 175203.	0.6	5
36	Investigation of excited state proton transfer mechanism for 2-(benzo[d]thiazol-2-yl)naphthalene-1,3-diol in different solvents. Chemical Physics, 2020, 538, 110914.	0.9	6

#	Article	IF	CITATIONS
	Exploring reaction mechanism and vibrational excitation effect in HÂ+ÂCH(<mml:math) 0.784314="" 1="" etqq1="" rgb<="" td="" tj=""><td>[/Overlock</td><td>2 10 Tf 50 7</td></mml:math)>	[/Overlock	2 10 Tf 50 7
37		1.2	4
	reaction. Chemical Physics Letters, 2020, 749, 137398.		
38	Dynamics of H(² <i>S</i>) + CH(<i>X</i> ² Î) reactions based on a new CH ₂ (\${ilde{X}}^{3}A^{primeprime} \$) surface via extrapolation to the complete basis set limit. Journal of Physics B: Atomic, Molecular and Optical Physics, 2020, 53, 095202.	0.6	6
39	Electric Field-Modulated Surface Enhanced Raman Spectroscopy by PVDF/Ag Hybrid. Scientific Reports, 2020, 10, 5269.	1.6	11
40	The role of intermolecular interactions in regulating the thermally activated delayed fluorescence and charge transfer properties: a theoretical perspective. Journal of Materials Chemistry C, 2020, 8, 8601-8612.	2.7	22
41	Mid-infrared Q-switch performance of ZrC. Photonics Research, 2020, 8, 1857.	3.4	6
42	An investigation into self-pulsing behavior in an Er-doped ring laser. Applied Physics Express, 2020, 13, 112006.	1.1	3
43	Quantum state-to-state dynamics of O ⁺ + H ₂ (<i>ν</i> = 0, j = 0) → OH ⁺ (<i>ν</i> [′] , j [′]) + H reaction on a global potential energy surfac Europhysics Letters, 2019, 126, 53001.	ഇ.7	8
44	The substituent effect on the excited state intramolecular proton transfer of 3-hydroxychromone*. Chinese Physics B, 2019, 28, 093102.	0.7	13
45	HCS(A2A″)-based insights into the effect of vibrational excitation on the reactions C+SHÂ(v =) Tj ETQq1 1 0.78	4314 rgBT 0.6	0verlock
46	The mechanism of the excited-state proton transfer of Salicylaldehyde azine and 2,2'-[1,4-Phenylenebis{(E)- nitrilomethylidyne}] bisphenol: Via single or double proton transfer. Spectrochimica Acta - Part A: Molecular and Biomolecular Spectroscopy, 2019, 223, 117321.	2.0	8
47	Accurate global potential energy surface for SiH2+(X2A1) and quantum dynamics of related reaction H(2S) + SiH+(X1Σ+). Journal of Chemical Physics, 2019, 150, 224304.	1.2	14
48	The novel excited state intramolecular proton transfer broken by intermolecular hydrogen bonds in HOF system. Spectrochimica Acta - Part A: Molecular and Biomolecular Spectroscopy, 2019, 219, 164-172.	2.0	36
49	Stereo-dynamics of the reaction C + SH(D,T)(v = 0, j = 0) → H(D,T) + CS based on a rece energy surface. Computational and Theoretical Chemistry, 2019, 1155, 82-89.	ent excited 1.1	l state po <mark>ce</mark>
50	Studies of the Coriolis coupling effect on reaction dynamics of \${m{H}}({}^{2}{m{S}})+{m{O}}{{m{H}}^{+} ightarrow {m{O}}({}^{3}{m{P}})+{{m{H}}_{2}^{+}({{m{m X}}}^{2}{{m{Sigma }}}_{{m{g}}^{+})\$ using the time dependent wave packet method. Journal of Physics B: Atomic, Molecular and Optical Physics, 2019, 52, 105201.	0.6	0
51	Field-free alignment dynamics of FCN molecule induced by a terahertz half-cycle pulse. Europhysics Letters, 2019, 125, 33001.	0.7	12
52	Investigation on the mechanism of ESIPT of 2-hydroxy-1-naphthaldehyde-(4-pyridinecarboxylic)-hydrazone and detection of Al ³⁺ ion. Canadian Journal of Physics, 2019, 97, 721-725.	0.4	16
53	A detecting Al3+ ion luminophor 2-(Anthracen-1-yliminomethyl)-phenol: Theoretical investigation on the fluorescence properties and ESIPT mechanism. Spectrochimica Acta - Part A: Molecular and Biomolecular Spectroscopy, 2019, 208, 309-314.	2.0	22
54	Doping-induced negative differential conductance enhancement in single-molecule junction. Physica F: Low-Dimensional Systems and Nanostructures, 2019, 106, 270-276	1.3	17

#	Article	IF	CITATIONS
55	Theoretical Study on the Sensing Mechanism of Novel Hydrazine Sensor TAPHP and Its ESIPT and ICT Processes. Frontiers in Chemistry, 2019, 7, 932.	1.8	24
56	A theoretical study on the ESPT mechanism for a novel Bisâ€HPBT fluorophore. Journal of Physical Organic Chemistry, 2018, 31, e3821.	0.9	10
57	Globally Accurate Potential Energy Surface for HCS(A ² A″) by Extrapolation to the Complete Basis Set Limit. Journal of Physical Chemistry A, 2018, 122, 4390-4398.	1.1	17
58	Accurate global potential energy surface for the ground state of CH ₂ ⁺ by extrapolation to the complete basis set limit. RSC Advances, 2018, 8, 13635-13642.	1.7	16
59	Electrically enhanced hot hole driven oxidation catalysis at the interface of a plasmon–exciton hybrid. Nanoscale, 2018, 10, 5482-5488.	2.8	110
60	The manifestation of vibrational excitation effect in reactions C + SH(<i>v</i> = 0–20, <i>j</i> = 0) \$ ightarrow \$ H + CS, S + CH. Journal of Physics B: Atomic, Molecular and Optical Physics, 2018, 51, 065202.	0.6	11
61	Theoretical investigation on excited state intramolecular proton transfer of 1-aryl-2-(furan-2-yl) butane-1, 3-diones substitutions. Journal of Molecular Structure, 2018, 1173, 341-344.	1.8	20
62	A global potential energy surface for H ₂ <i>S</i> ⁺ <i>(X ⁴A′′)</i> and quasi-classical trajectory study of the S ⁺ <i>(⁴S)</i> + H ₂ <i>(X¹Σ⁺_g)</i> reaction. Molecular Physics, 2018, 116, 129-141.	0.8	19
63	Exciton-plasmon coupling interactions: from principle to applications. Nanophotonics, 2018, 7, 145-167.	2.9	164
64	A theoretical investigation on excited-state single or double proton transfer process for aloesaponarin I. Canadian Journal of Chemistry, 2018, 96, 83-88.	0.6	12
65	Novel potential energy surface-based quantum dynamics of ion–molecule reaction \${{m{O}}}^{+}+{{m{D}}}_{2}o {mathrm{OD}}^{+}+{m{D}}\$. Chinese Physics B, 2018, 27, 043104.	0.7	7
66	Quantum dynamics calculations for O+ + H2 (vi = 0, ji = 0) → OH+ + H ion–molecule reaction on a new potential energy surface. European Physical Journal D, 2018, 72, 1.	0.6	4
67	Accurate potential energy surface of H2S+(X2A″) via extrapolation to the complete basis set limit and its use in dynamics study of S+(D2)+H2(X1Σg+) reaction. Journal of Chemical Physics, 2018, 149, 154303.	1.2	19
68	Exciton–plasmon hybrids for surface catalysis detected by SERS. Nanotechnology, 2018, 29, 372001.	1.3	17
69	Excited state intramolecular proton transfer mechanism of o-hydroxynaphthyl phenanthroimidazole. Chinese Physics B, 2018, 27, 023103.	0.7	19
70	The order of multiple excited state proton transfer in ternary complex of norharmane and acetic acids. Spectrochimica Acta - Part A: Molecular and Biomolecular Spectroscopy, 2018, 202, 30-35.	2.0	20
71	Exploring the reaction dynamics of O(³ P)+ (X ²)→OH ⁺ (X ³ Σ ^{â~'})+ H(² S) reaction with timeâ€dependent wave packet method. International Journal of Quantum Chemistry, 2017, 117, e25343.	1.0	11
72	A globally accurate potential energy surface of \$\$mathrm{HS_2}{(A,^2A^prime)}\$\$ HS 2 (A 2 A ′) and studies on the reaction dynamic of \$\$mathrm{H}(^2mathrm{S})+mathrm{S_2}(a,^1{varDelta }_g)\$\$ H (2 S) + S 2 (a 1 Δ g). Theoretical Chemistry Accounts, 2017, 136, 1.	0.5	9

#	Article	IF	CITATIONS
73	Recent advances in surface plasmon-driven catalytic reactions. RSC Advances, 2017, 7, 31189-31203.	1.7	58
74	Effect of H2O Adsorption on Negative Differential Conductance Behavior of Single Junction. Scientific Reports, 2017, 7, 4195.	1.6	8
75	Electrooptical Synergy on Plasmon–Excitonâ€Codriven Surface Reduction Reactions. Advanced Materials Interfaces, 2017, 4, 1700869.	1.9	91
76	Accurate Theoretical Study of LiS Radical and Its Singly Charged Cation and Anion in their Ground Electronic State. Chinese Journal of Chemical Physics, 2017, 30, 128-134.	0.6	4
77	Solvent Effects on Two-Photon Absorption of Alkyne and Alkene <i>Ï€</i> -bridging Chromophores. Chinese Journal of Chemical Physics, 2017, 30, 63-70.	0.6	2
78	The stereodynamics study on the isotopic substitution C + SH(D, T) → H(D, T) + CS reactions on the new HCS(<i>X</i> ² A′) potential energy surface. Canadian Journal of Physics, 2017, 95, 1219-1224.	0.4	7
79	by scaling the external correlation. Chinese Physics B, 2016, 25, 053101.	0.7	6
80	Globally accurate potential energy surface for the ground-state HCS(X2A′) and its use in reaction dynamics. Scientific Reports, 2016, 6, 37734.	1.6	15
81	Particle Densities of the Atmospheric-Pressure Argon Plasmas Generated by the Pulsed Dielectric Barrier Discharges. Plasma Science and Technology, 2016, 18, 1081-1088. Coriolis coupling effects in the cmml:math xmlns:mml="http://www.w3.org/1998/Math/MathMI "	0.7	8
82	Coriolis coupling effects in the <mml:math <br="" xmlns:mml="http://www.w3.org/1998/Math/MathML">altimg="si3.gif" overflow="scroll"><mml:mrow><mml:mtext>H</mml:mtext><mml:mo>+</mml:mo><mml:msub><mml:mtext>L stretchy="false">(<mml:msup><mml:mtext>X</mml:mtext><mml:mn>1</mml:mn></mml:msup><m< td=""><td></td><td></td></m<></mml:mtext></mml:msub></mml:mrow></mml:math>		
83	Accurate theoretical study on the ground and first-excited states of Na2: potential energy curves, spectroscopic parameters, and vibrational energy levels. Canadian Journal of Physics, 2016, 94, 1259-1264.	0.4	6
84	Numerical simulation of evolution features of the atmospheric-pressure CF4 plasma generated by the pulsed dielectric barrier discharge. European Physical Journal D, 2016, 70, 1.	0.6	14
85	Theoretical Analysis on Optical Limiting Properties of Newly Synthesized Graphene Oxide-Porphyrin Composites. Chinese Journal of Chemical Physics, 2015, 28, 257-262.	0.6	4
86	Accurate <i>ab initio</i> -based analytical potential energy function for S ₂ (ã) Tj ETQq0 0 0 rgBT / 24, 013101.	Overlock 0.7	10 Tf 50 227 11
87	Accurate potential energy curve and spectroscopic properties of S ₂ (<i>b</i> ¹ â^< _{<i>g</i>} ⁺) via extrapolation to the complete basis set limit. Physica Scripta, 2015, 90, 035403.	1.2	11
88	Effect of thiophene rings on UV/visible spectra and non-linear optical (NLO) properties of triphenylamine based dyes: a quantum chemical perspective. Journal of Physical Organic Chemistry, 2015, 28, 418-422.	0.9	99
89	The quantum dynamics of the reactions N+H ₂ (HD,D ₂) and their vibrational excitation effect. International Journal of Quantum Chemistry, 2015, 115, 231-238.	1.0	6
90	Globally accurate <i>ab initio</i> based potential energy surface of H ₂ O ⁺ (<i>X</i> ⁴ A″). Chinese Physics B, 2015, 24, 063101.	0.7	17

#	Article	IF	CITATIONS
91	Accurate adiabatic potential energy surface for 12A′ state of FH2 based on ab initio data extrapolated to the complete basis set limit. European Physical Journal D, 2015, 69, 1.	0.6	8
92	Cross sections for vibrational inhibition at low collision energies for the reaction H + Li2(X1Σ g +) → Li + LiH (X1Σ+). European Physical Journal D, 2015, 69, 1.	0.6	32
93	A typical slow reaction H(² S) + S ₂ (<i>X</i> ³ Σ ^{â^'}) Tj ETQ calculation. Chinese Physics B, 2014, 23, 073101.	2q1 1 0.78 0.7	84314 rgBT 8
94	Variation of Two-Photon Absorption Cross Sections and Optical Limiting of Compounds Induced by Static Electric Field. Chinese Journal of Chemical Physics, 2014, 27, 259-264.	0.6	2
95	Dynamical properties of S(³ P) + HD reaction on 1 ³ <i>A</i> ″state and their quantum wavepacket calculation. International Journal of Quantum Chemistry, 2014, 114, 748-754.	1.0	8
96	Accurate ab initio-based DMBE potential energy surface for HLi2(X  2A′) via scaling of the external correlation. European Physical Journal D, 2014, 68, 1.	0.6	13
97	The NLO properties of hybrid materials based on molybdate/hexamolybdate derivatives: A theoretical perspective for electro-optic modulation. Synthetic Metals, 2014, 198, 277-284.	2.1	5
98	Effect of reagent vibrational excitation on reaction S(3P)+D2 in 3A″ and 3A′ states. Computational and Theoretical Chemistry, 2014, 1039, 15-20.	1.1	7
99	Effect of π-conjugation spacer (CC) on the first hyperpolarizabilities of polymeric chain containing polyoxometalate cluster as a side-chain pendant: A DFT study. Computational and Theoretical Chemistry, 2012, 994, 34-40.	1.1	138
100	<i>Ab initio</i> -based double many-body expansion potential energy surface for the first excited triplet state of the ammonia molecule. Journal of Chemical Physics, 2012, 136, 194705.	1.2	25
101	Accurate Double Many-Body Expansion Potential Energy Surface for Ground-State HS ₂ Based on ab Initio Data Extrapolated to the Complete Basis Set Limit. Journal of Physical Chemistry A, 2011, 115, 5274-5283.	1.1	30
102	Potential Energy Surface for Ground-State H2S via Scaling of the External Correlation, Comparison with Extrapolation to Complete Basis Set Limit, and Use in Reaction Dynamics. Journal of Physical Chemistry A, 2009, 113, 9213-9219.	1.1	25
103	Accurate <i>ab initio</i> double many-body expansion potential energy surface for ground-state H2S by extrapolation to the complete basis set limit. Journal of Chemical Physics, 2009, 130, 134317.	1.2	50
104	A comparison of single-reference coupled-cluster and multi-reference configuration interaction methods for representative cuts of the potential energy surface. Computational and Theoretical Chemistry, 2008, 859, 22-29.	1.5	14
105	Solvent effects on two-photon absorption cross sections of a newly synthesized polymerization initiator. Computational and Theoretical Chemistry, 2006, 772, 75-79.	1.5	11
106	Dynamical behavior of ultra-short laser pulse in a cascade three-level molecular system. Wuli Xuebao/Acta Physica Sinica, 2006, 55, 1803.	0.2	7
107	Quantum and Quasiclassical Dynamics of the \${mf C}(f ^3P)\$ + \${mf H_2}(f ^1Sigma_g^+)\$ \$ightarrow\$ \${mf H}(f ^2S)\$ + \${mf CH}(f ^2Pi)\$ reaction: Coriolis Coupling Effects and Stereodynamics. Chinese Physics B, 0, , .	0.7	1